



# Local atomic order in the vicinity of Cu<sub>2</sub> dumbbells in TbCu<sub>7</sub>-type YCu<sub>6.576</sub> studied by Bragg and total scattering techniques

Radovan Černý<sup>a,\*</sup>, Yaroslav Filinchuk<sup>a,b</sup>, Stefan Brühne<sup>c</sup>

<sup>a</sup>Laboratory of Crystallography, University of Geneva, 24 Quai Ernest Ansermet, CH-1211 Geneva 4, Switzerland

<sup>b</sup>Swiss-Norwegian Beam Lines at ESRF, BP-220, F-38043 Grenoble, France

<sup>c</sup>Institute of Physics, Goethe University Frankfurt, Max-von-Laue-Str., 1, D-60438 Frankfurt am Main, Germany

## ARTICLE INFO

### Article history:

Received 6 October 2008

Received in revised form

23 February 2009

Accepted 10 March 2009

Available online 11 April 2009

### Keywords:

A. Intermetallics, miscellaneous

B. Crystallography

F. Diffraction

B. Order/disorder transformations

D. Site occupancy

## ABSTRACT

The crystal structure of YCu<sub>6.576</sub>, a hyperstoichiometric substitution variant of the CaCu<sub>5</sub>-structure type, was shown to contain Cu<sub>2</sub> dumbbells replacing Y-atoms in a fraction  $s = 0.19$  in the formula Y<sub>1-s</sub>Cu<sub>5+2s</sub>. The structure type TbCu<sub>7</sub> is assigned to the disordered structure (*P6/mmm*,  $a = 4.96$  Å,  $c = 4.15$  Å). The local order in the vicinity of the Cu<sub>2</sub>-dumbbells has been derived from total scattering X-ray synchrotron data via refinement of the atomic pair distribution function (PDF). The coordinating Cu<sub>6</sub>-hexagon around the dumbbell site shows a shrinkage of 0.33(1) Å w.r.t. the equivalent environment of the Y-atom. No adjacent Y-atoms are substituted but a hexagonal arrangement of Cu<sub>2</sub>-dumbbells, separated at least by the vectors  $\sqrt{3}\mathbf{a}$  and  $\sqrt{3}\mathbf{b}$  exists in layers perpendicular to  $\mathbf{c}$ . The stacking along [001] is random and can be modeled locally from the PDF data consistent with both *ab*- and *abc*-type stacking. Therefore, the local order is comparable to that in Ni<sub>17</sub>Th<sub>2</sub>- and Th<sub>2</sub>Zn<sub>17</sub>-structure types. X-ray single crystal analysis and Rietveld refinements of neutron- and X-ray powder data (Bragg diffraction data) of YCu<sub>6.576</sub> are consistent with the findings from local crystallography (total scattering data) answering a long-standing question in disordered CaCu<sub>5</sub>-type based intermetallic structure variants.

© 2009 Elsevier Ltd. All rights reserved.

## 1. Introduction

Within the plethora of intermetallic phases, the CaCu<sub>5</sub>-structure type [1] is one of the most frequent representatives of AB<sub>5</sub> compositions [2]. In this formula, *A* may be a lanthanide, alkaline earth, or transition element, *B* a *d*- or *p*-block element. Also their ternary derivatives are of interest for various technological applications such as permanent magnets – mind the super magnet SmCo<sub>5</sub> – and hydrogen storage materials [2]. The CaCu<sub>5</sub>-structure type comprises six atoms in a primitive hexagonal cell consistent with space group symmetry *P6/mmm*, Pearson symbol *hP6*; *a* and *c* lattice parameters are of comparable dimension about 5 Å. The atom *A* is located at Wyckoff site 1*a* and the *B* atoms at 2*c* and 3*g* (Fig. 1a). Thus the structure can be described in terms of two types of nets stacked along the  $\mathbf{c}$  vector: in the basal plane ( $z = 0$ ) we find a regular honeycomb net of *B*-atoms the hexagons of which are centred by *A*-atoms (Fig. 1b) and at  $z = 1/2$  a *kagomé* net built of *B*-atoms (Fig. 1c).

Basing on this generic AB<sub>5</sub> structure type, a number of related structure types are known: Replacing *A*-atoms by *B*<sub>2</sub> dumbbells in

\* Corresponding author.

E-mail address: [radovan.cerny@unige.ch](mailto:radovan.cerny@unige.ch) (R. Černý).

a fraction  $s$  (concentration w.r.t. *A*-atoms) leads to the formulae A<sub>1-s</sub>B<sub>5+2s</sub>. In this way, stoichiometries from AB<sub>5</sub> to AB<sub>9.5</sub> can be realized. A local view on this substitution is given in Fig. 1d–f. After substitution, three kinds of situations are possible: (i) The substituted atoms order perfectly, this leads to superstructures of the CaCu<sub>5</sub> substructure. (ii) The replacement is totally random and the overall symmetry of the CaCu<sub>5</sub> type is retained. (iii) Disorder is contained in a superstructure, *i.e.* a combination of (i) and (ii).

The ordered substitution (i) with  $s = 1/3$  leads to the so-called **2:17** structures: hexagonal Th<sub>2</sub>Ni<sub>17</sub> type (*P6<sub>3</sub>/mmc*;  $a' = \sqrt{3}a$ ,  $c' = 2c$  [3]) and rhombohedral Th<sub>2</sub>Zn<sub>17</sub> type (*R-3m*;  $a' = \sqrt{3}a$ ,  $c' = 3c$  [4]) having the common subcell (*a*, *c*). These structures can be regarded as hexagonal *ab* (Th<sub>2</sub>Ni<sub>17</sub> type) or rhombohedral *abc* (Th<sub>2</sub>Zn<sub>17</sub> type) stacking variants of idealized CaCu<sub>5</sub>-like structural slabs (Fig. 1b and e) in which the *B*<sub>2</sub> dumbbells are ordered in a hexagonal arrangement [5] (see Fig. 2, middle part). It was shown in Ref. [6] that the substitution, if fully disordered (case ii), results in the structure type TbCu<sub>7</sub> (*P6/mmm*;  $a' = a$ ,  $c' = c$  [7]) where  $s$  can vary between 0 and 1/3 (see Results and discussion). A partially disordered Th<sub>2</sub>Ni<sub>17</sub> structure (case iii) gives the structure type LuFe<sub>9.5</sub> (*P6<sub>3</sub>/mmc*;  $a' = \sqrt{3}a$ ,  $c' = 2c$ ) [8]. Partially disordered Th<sub>2</sub>Zn<sub>17</sub> structure yields the structure type PrFe<sub>7</sub> (*R-3m*,  $a' = \sqrt{3}a$ ,  $c' = 3c$  [9]). In both cases  $s$  can be higher or lower than 1/3 depending on

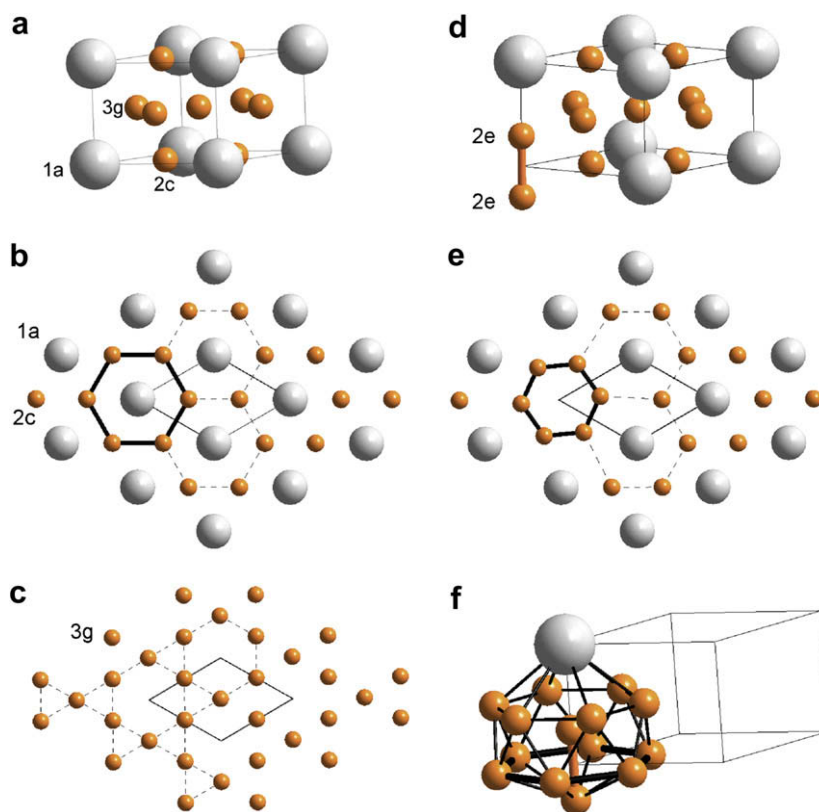


**Fig. 1.** Substitutions in  $\text{CaCu}_5$ -type based structures. One **1:5H** hexagonal unit cell is outlined, the Wyckoff positions refer to space group  $P6/mmm$ . Left column (a–c): Parent structure  $\text{AB}_5$ ; (a) unit cell, A- (B-) atoms are represented by large (small) spheres; (b) the layer at  $z = 0$ , B-atoms form a honeycomb pattern, one hexagon of which is highlighted; (c) the layer at  $z = 1/2$  made of B-atoms arranged in a *kagomé* pattern. Right column (d–f): Substitution of an A-atom by a  $B_2$  dumbbell; (d) unit cell view; (e) the layer at  $z = 0$ : the missing A-atom causes a distortion of the B-atom honeycomb net; (f) the shrunken hexagon highlighted in the local coordination polyhedron about one dumbbell B-atom.

the system. Other substitution variants with higher  $s$  exist too (see [Results and discussion](#)), but are not relevant in our study. According to their unit cell dimensions and translational symmetries, we will refer below to the compounds with  $\text{CaCu}_5$  and  $\text{TbCu}_7$  structures as **1:5H**, to the compounds with  $\text{Th}_2\text{Ni}_{17}$  and  $\text{LuFe}_{9.5}$  structures as **2:17H**, and to the compounds with  $\text{Th}_2\text{Zn}_{17}$  and  $\text{PrFe}_7$  structures as **2:17R**. More complex situations may occur: recently a polytypic

intergrowth of two 2:17 domains, H and R, was observed in a  $\text{Yb}_{2-x}(\text{Fe,Ga})_{17+2x}$  single crystal [5].

Whereas the local situation around  $B_2$  dumbbells in the ordered variants (i) is clear from classical crystal structure analysis, it remains obscure in the case of disorder (ii, iii). Within the **1:5H** cell in  $P6/mmm$ , the  $B_2$  dumbbell (site 2e) replacing A atom (site 1a) is likely to be correlated with the B atom displacements from 2c to 6l

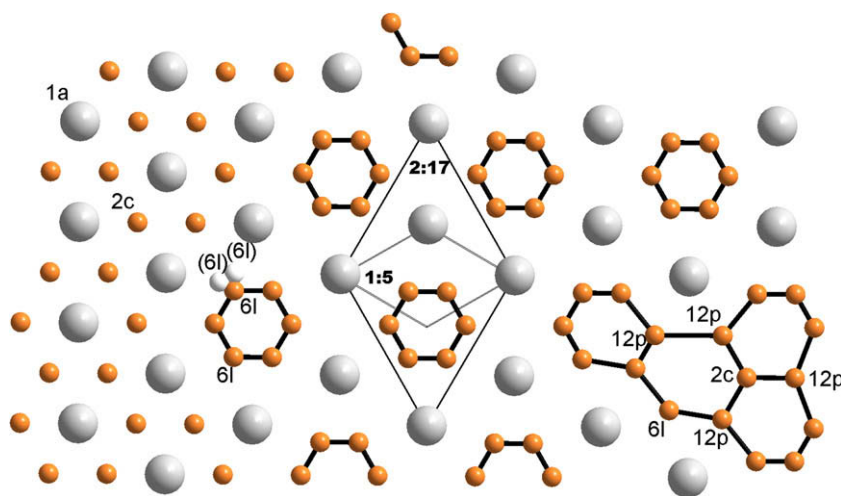


**Fig. 2.** Different situations in the  $z = 0$  layer (w.r.t. **1:5H** cell,  $P6/mmm$ ) of a substituted  $\text{AB}_5$   $\text{CaCu}_5$ -type based structure. Left-hand part: non-substituted **1:5H** cell, large A-atoms in 1a, small B-atoms in 2c. Middle part: substitution of A by  $B_2$  dumbbells creates holes at  $z = 0$ , B-atoms in this plane shift to 6l sites forming shrunken hexagons. In  $P6/mmm$  “ghost atoms” at (6l) are generated by space group symmetry at positions more distant from the hole (only drawn once). The **1:5H** unit cell is outlined, primitive hexagonal ordering of holes generates a  $\sqrt{3} \times \sqrt{3}$  superstructure **2:17** (H –  $P6_3/mmc$  or R –  $R-3m$  depends on the stacking sequence). Right-hand part: adjacent holes provoke shifts of B-atoms to 12p and back to 2c sites as observed in  $\text{LuFe}_{9.5}$ .

Wyckoff site (i.e. a shrinkage or expansion of  $B$  atom honeycomb hexagons in the immediate vicinity of now empty  $A$  atom sites, compare Fig. 1b to Fig. 1e). A model of correlated  $B$  atom displacements from  $2c$  to  $6l$  Wyckoff site in **1:5H** structure was first proposed in Ref. [10] for  $\text{YbCu}_{6.5}$ , although no structure refinement has been performed. Such correlated  $B$  atom displacements are observed for example in  $\text{Sm}_2(\text{Fe}_{1-x}\text{Al}_x)_{17}$  (**2:17R**, structure type  $\text{Th}_2\text{Zn}_{17}$  [11]) where these displacements are ordered and the hexagons of  $B$  atoms shrink around the  $B_2$  dumbbell. To our knowledge, the first complete structure refinement on the  $\text{AB}_{5+x}$  compound yielding both the dumbbell substitution ratio and the fraction of  $B$  atoms displaced from site  $2c$  to site  $6l$  was performed in Ref. [12] by single crystal neutron diffraction on  $\text{SmCo}_5$ . In Ref. [8] the authors have observed that in  $\text{LuFe}_{9.5}$  the displacement of  $B$  atoms from site  $2c$  can occur also towards the site  $12p$  (w.r.t. **1:5H** subcell), when two or three neighboring  $A$  atoms are replaced by  $B_2$  dumbbells (see Fig. 2, right-hand part).

The work on hyperstoichiometric  $\text{LaNi}_{5+x}$  in Ref. [13] (**1:5H**) confirms the structural model of correlated  $B$  atom displacements from  $2c$  to  $6l$  site [10], and for the first time provides complete agreement between structural parameters such as dumbbell substitution ratios and fractions of displaced atoms, and independent measurements of composition and mass density. No displacement of Ni atoms from  $2c$  to  $12p$  site was observed. Interatomic distances suggest that the local Ni atom displacements from  $2c$  to  $6l$  site should occur in directions towards the  $\text{Ni}_2$  dumbbell rather than in the opposite direction [13]. However, the absolute direction of the shifts (towards or from the dumbbell) cannot be clarified from Bragg intensities because due to the translational symmetry local 3-fold symmetry is pretended (see “ghost atoms” in Fig. 2 or Fig. 4 in Ref. [13]). Only a study of diffuse intensity will resolve that problem.

Therefore, we have studied the question of the local  $B$ -atom order around a  $B_2$  dumbbell on  $\text{YCu}_{5+x}$  which also crystallizes in the **1:5H** type structure. A combination of Bragg (X-ray single crystal, powder, and neutron powder diffraction) and total scattering (X-ray powder) techniques was used. Questions to be answered are: Is the geometry of the  $B_2$  dumbbells comparable to that in the ordered **2:17** phases? How is the local symmetry affected by the substitution of an  $A$ -atom by a  $B_2$ -dumbbell? What is the correlation among neighboring  $B_2$  dumbbells like, e.g. is there a minimum distance between the dumbbells or is there total randomness? We have

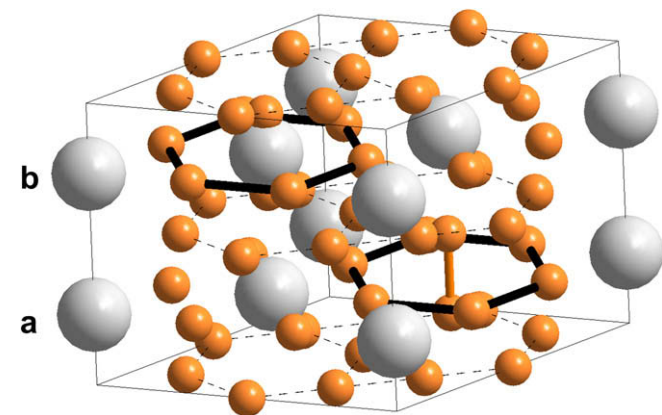


**Fig. 3.** Refinement box **2:17H** for PDF refinement, yttrium shown as large, copper as smaller spheres. Two yttrium sites (Y1a and Y1a') from the Table 3 correspond to Y atoms from the structural slabs a and b, respectively. The *kagomé* nets at  $z=0$  are stacked primitively along  $[001]$ . Layers a at  $z=1/4$  and b at  $z=3/4$  contain the substituted Y-atoms and correspond to the layer at  $z=0$  in the **1:5H** cell. The highlighted  $\text{Cu}_6$ -hexagons correspond to those in Figs. 1b, e, f and 2.

chosen the  $\text{YCu}_{5+x}$  compound, because high dumbbell concentrations can be easily obtained and single phase samples prepared. Hyperstoichiometric  $\text{YCu}_{5+x}$  was studied in Refs. [7] and [14] before: The existence of a large homogeneity range between  $\text{YCu}_5$  (obtained only by splat cooling) and  $\text{YCu}_7$  was suggested in Ref. [7]. The most rich concentration of dumbbells was observed as  $s=0.157(3)$  and corresponds to the refined composition  $\text{YCu}_{6.433}$  [14].

Bragg data for  $\text{YCu}_{5+x}$  were analyzed using classical single crystal and Rietveld refinements revealing the *average long range* structure which contains partially occupied sites. A total scattering experiment samples Bragg and diffuse scattering data simultaneously – the latter contains direct information on disorder [15]. The atomic pair distribution function (PDF, [15]) was generated from the X-ray powder total scattering data and analyzed by refinements of test-models describing directly the *local, i.e. non-periodic* structure. Recently, the PDF method was successfully used in the field of intermetallics to refine the local structure of icosahedral quasicrystals [16,17] and of the complex metallic alloy  $\beta\text{-Al}_3\text{Mg}_2$  (cF1168, [18]). Here we combine PDF from total scattering with classical Bragg experiments to get a coherent answer to the problem of local structure in substituted disordered  $\text{CaCu}_5$ -type based alloys.

## 2. Experimental

### 2.1. Synthesis

The alloy was prepared from the mixture of elements (Y – 99.99%, Ventron; Cu – 99.999%, Alfa Aesar). The nominal composition was  $\text{YCu}_{6.576}$  giving  $s=0.184$ . The sample (3 g) was melted by arc, with subsequent five re-meltings, then re-melted in the induction furnace, keeping it in the liquid state for 1 min. The alloy was then sealed in a 9 mm quartz tube and annealed for one month at  $800^\circ\text{C}$ , and quenched into cold water. Single crystals were found on the surface of the sample. Assuming weighting errors (0.1%) and evaporation losses during melting (0.2%) the precision of the nominal dumbbells concentration in the alloy is estimated to be 0.3%.

### 2.2. Data collection and analysis of Bragg scattering

High resolution synchrotron powder pattern used for Rietveld refinement was measured at the SNBL, ESRF Grenoble (sample in a 0.4 mm glass capillary, room temperature,  $\lambda=0.49949\text{ \AA}$ ,  $Q_{\text{max}}=13\text{ \AA}^{-1}$ , 6-crystal analyzer detector), and neutron powder pattern used for Rietveld refinement was measured on the diffractometer D2B, ILL Grenoble (sample in a 10 mm vanadium container, room temperature,  $\lambda=1.594\text{ \AA}$ ,  $Q_{\text{max}}=7.76\text{ \AA}^{-1}$ ). Another synchrotron powder pattern which was then used for PDF analysis was measured at the Swiss Light Source (SLS), PSI Villigen ( $\lambda=0.43350\text{ \AA}$ ,  $Q_{\text{max}}=23\text{ \AA}^{-1}$ , curved Si-strip detector Mythen 2 [19]). A single crystal was cut out from sticks on the surface of the alloy and measured on Stoe IPDS I diffractometer at 150 K using  $\text{Mo K}\alpha$  radiation. The data collection parameters are given in the Table 1.

The Rietveld refinement was done with the program Fullprof [20] using the synchrotron and neutron data separately. The background was modeled by the Fourier filtering technique, and the displacement factors of all atoms were refined isotropically. The single crystal data analysis was done with the program SHELXL97 [21], the displacement factors of all atoms were refined anisotropically with the exception of the Cu atoms on the sites  $2c$  and  $6l$  which were refined isotropically. More details about the parameters of Rietveld and single crystal refinements are given in Table 1. The occupancy factors for different Wyckoff sites in the **1:5H**

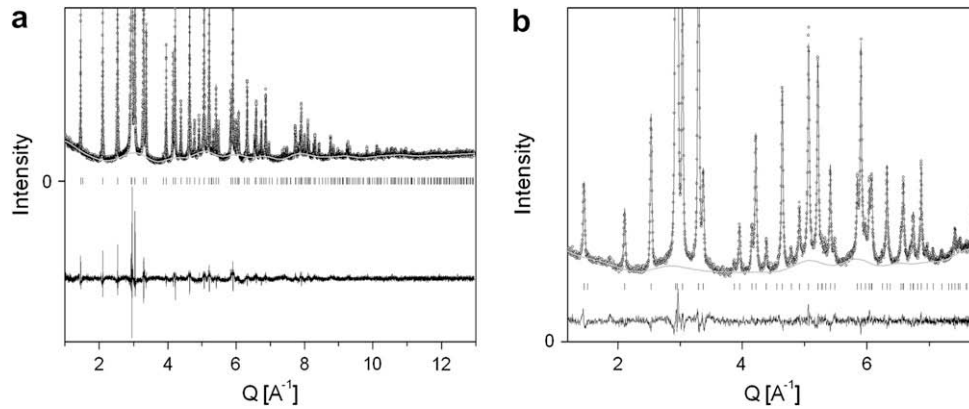


**Fig. 4.** Rietveld plot of the synchrotron (a) and neutron (b) data. The background modeled by Fourier filtering is drawn as light grey curve, and shows similar features around  $Q = 3$ , 5 and  $6 \text{ \AA}^{-1}$  for both data. The difference curve is shown at the bottom in both plots.

structure were set in all Rietveld and single crystal refinements according to the model of correlated shift of Cu atom hexagons in the immediate vicinity of  $\text{Cu}_2$  dumbbell as follows:

$$1a : 1 - s, 2c : 1 - 3s, 3g : 1, 2e : s, 6l : s \quad (1)$$

where  $s$  corresponds to the concentration of  $\text{Cu}_2$  dumbbells on the Y site.

### 2.3. Analysis of total scattering

The observed reduced PDF was obtained (program PDFgetX2 [22]) from the synchrotron powder diffraction data via a *sine* Fourier transform of the normalized total scattering structure function  $S(Q)$  (see Ref. [15])

$$G(r) = 4\pi r [\rho(r) - \rho_0] = \frac{2}{\pi} \int_0^{\infty} Q[S(Q) - 1] \sin(Qr) dQ \quad (2)$$

where  $\rho(r)$  is the microscopic pair density,  $\rho_0$  is the average number density and  $Q$  is the magnitude of the scattering vector  $Q$ . For elastic scattering it is  $Q = |Q| = 4\pi \sin(\theta)/\lambda$  with  $2\theta$  being the scattering angle and  $\lambda$  the wavelength of the radiation used. The observed PDF was used in the refinement of the structural model (program PDFgui [23]). The calculated PDF is obtained from the structural model by the relation

$$G_{\text{calc}}(r) = \frac{1}{r} \sum_{ij} \left[ \frac{f_i(0)f_j(0)}{\langle f \rangle^2} \delta(r - r_{ij}) \right] - 4\pi r \rho_0 \quad (3)$$

where the sum goes over all pairs of atoms  $i$  and  $j$  within the model crystal separated by  $r_{ij}$  [15]. The X-ray scattering power of atom  $i$  is  $f_i$  and  $\langle f \rangle$  is the average scattering power of the sample. As the X-ray scattering power of the atoms is  $Q$ -dependent equation (2) is not exactly valid. The weighting factors of Cu–Cu, Cu–Y and Y–Y correlations for partial structure functions in equation (3) are also  $Q$ -dependent. Fourier transformation then yields a convolution of the weighting factors and partial structure functions. However, an approximation of  $f(Q)$  by  $f(0)$  is usually accepted as precise enough [15], because the  $Q$ -dependences of the weighting factors are negligible small. It is then possible to calculate the  $G(r)$  from the models and compare it with experimental  $G(r)$  in  $r$ -space.

To model the local order, periodic refinement boxes of local symmetry, other than derived from the Bragg experiment, have to be set up. These refinement boxes allow to refine ordering with *local* symmetries which are not compatible with the *long range* translational symmetry. Three PDF refinement boxes were created from the **1:5H** structure with the atomic coordinates and lattice parameters as resulted from the Rietveld synchrotron refinement: (i) **1:5H** box identical to the **1:5H** structure from the Rietveld, (ii) **2:17H** box with the **1:5H** structure transformed to the **2:17H** cell with  $a' = \sqrt{3}a$  and  $c' = 2a$ , and (iii) **2:17R** box with the **1:5H**

**Table 1**

Parameters of Rietveld synchrotron and neutron, of pair distribution function (PDF) synchrotron and of single crystal X-ray data analyses for  $\text{YCu}_{6.576}$ . Results of three different PDF refinement boxes (**1:5H**, **2:17H** and **2:17R**) are given.

	Synchrotron			Neutrons Rietveld	X-ray single crystal
	Rietveld	PDF 1:5H	PDF 2:17H		
Wavelength [Å]	0.49949	0.43350		1.594	0.71073
$Q_{\text{max}}$ [ $\text{\AA}^{-1}$ ]	13	23		7.76	9.60
Number of independent reflections	82	–		51	94
$N_{\text{ref}}/\text{param.}$	10	–		5.7	6.3
$R_{\text{int}}$	–	–		–	0.09
$a$ of 1:5H cell [Å]	4.96303(1)	4.96983(3)	4.96875(2)	4.96831(2)	4.9616(1)
$c$ of 1:5H cell [Å]	4.13745(1)	4.15640(7)	4.15521(7)	4.15753(7)	4.1360(1)
$c/a$ of 1:5H cell	0.8337	0.8363	0.8363	0.8368	0.8336
$V$ [ $\text{\AA}^3$ ] of 1:5H cell	88.259(1)	88.91(1)	88.84(1)	88.88(1)	88.176(4)
$\chi^2$ , GooF	$\chi^2 = 2.11$	–	–	–	$\chi^2 = 1.17$
$R_B$ , $R_{\text{wp}}$ , $R_F$ , $wR_{F^2}$ [%]	$R_B = 4.5$ ; $R_{\text{wp}} = 13.2$	$R_{\text{wp}} = 16.9$	$R_{\text{wp}} = 16.6$	$R_{\text{wp}} = 17.4$	$R_B = 1.9$ ; $R_{\text{wp}} = 7.9$
$s$ – Concentration of dumbbells, nominal $s = 0.184(1)$	0.192(1)	0.186(1)	0.194(1)	0.176(1)	0.192(1)
Refined composition, nominal $\text{YCu}_{6.576(5)}$	$\text{YCu}_{6.663(6)}$	$\text{YCu}_{6.597(3)}$	$\text{YCu}_{6.689(3)}$	$\text{YCu}_{6.500(3)}$	$\text{YCu}_{6.663(6)}$
Effective multiplier SCOR: [24,25]	4.24; 5.23				2.09; 3.67

Note 1: The agreement factors  $R_{\text{wp}}$  for the PDF refinement seem to be too high compared to the refinement of Bragg intensities. In reality they are quite good; this issue was discussed in Ref. [32].

Note 2: The number of independent reflections in Rietveld refinement is estimated by program Fullprof [20] taking into account the reflections overlap.

structure transformed to the **2:17R** cell with  $a' = \sqrt{3}a$  and  $c' = 3a$ . We have constructed the PDF refinement boxes **2:17** as composed from two types of structural slabs:  $a$  being the fully ordered slab containing close packed  $\text{Cu}_2$  dumbbells (composition  $\text{Y}_2\text{Cu}_{17}$ ),  $b$  and  $c$  being the partly ordered slab containing close packed  $\text{Cu}_2$  dumbbells partly substituting Y atoms (composition  $\text{Y}_{3-s}\text{Cu}_{15+2s}$ ). The justification of using the close packing of  $\text{Cu}_2$  dumbbells is given in **Results and discussion**. The **2:17H** box contains  $a$  and  $b$  slab in the stacking  $ab$  (see Fig. 3), the **2:17R** box contains  $a$ ,  $b$  and  $c$  slab in the stacking  $abc$ . The structure was then expanded with the periodic boundary condition as it is common in the PDFgui program. The PDF refinement was done in all cases on the interval  $r = 1.8\text{--}20 \text{ \AA}$ . Lattice parameters, atomic coordinates, one occupancy factor (identical for  $b$  and  $c$  slab), five isotropic displacement parameters (corresponding to five independent atoms in the **1:5H** structure), scale factor and two factors describing the PDF peaks broadening due to the correlated thermal displacements (for more details see Ref. [15]) were refined. In addition, a  $2a$ ,  $2a$ ,  $3c$  **1:5H**-supercell has been used as another box to model inter-dumbbell correlations.

### 3. Results and discussion

The concentration of dumbbells  $s$  and the chemical formula refined from Rietveld, single crystal and PDF analyses are given in Table 1. The atomic parameters resulting from Rietveld analysis of synchrotron and neutron data, from the PDF analysis of synchrotron data (model **1:5H**) and from the single crystal data analysis are given in Table 2. Rietveld plots of synchrotron and neutron data are given in Fig. 4. The reduced structure function  $F(Q) = Q[S(Q) - 1]$  obtained from the synchrotron data is shown in Fig. 5. Plots of PDF refinement are shown in Fig. 6. The interatomic distances within the coordination polyhedron of each atom as obtained from the Rietveld analysis of synchrotron and neutron data, from the PDF analysis of synchrotron data (model **2:17H**) and from the single crystal data analysis are given in Table 3.

Please note that the values of all standard uncertainties given here are as they are calculated by respective refinement programs (SHELXL97 and FullProf). It is, however, well known that the precision of structural parameters is overestimated in the powder diffraction due to serial correlations in the observed data (individual points in the powder pattern) and non-accessibility of the goodness-of-fit parameter based on integrated intensities of individual reflections. Several theoretical models were proposed to correct this handicap, two of them are available in the program Fullprof: according to Refs. [24] and [25]. The multiplication factor SCOR for all standard uncertainties obtained from Rietveld refinement according to these two models is given in Table 1.

#### 3.1. Average structure of $\text{YCu}_{6.576}$ from Bragg scattering

The single crystal study was mainly aiming to detect any possible periodic ordering of dumbbells, which can be detected by appearance of superstructure reflections. No superstructure reflections were observed, thus indicating the true **1:5H** average structure.

The unrestrained Rietveld refinement of the **1:5H** structure using the Bragg synchrotron and neutron scattering provides coherent results which are in agreement with Refs. [7] and [14]. In particular, no displacement of Cu atoms from  $2c$  to  $12p$  site was observed, in agreement with our single crystal results. It means that there are no adjacent dumbbells present at any position in the structure (see Fig. 2, right-hand part). Consequently it follows that the dumbbells are packed hexagonally in the basal **1:5H** plane (see Fig. 2, middle part) when the concentration of dumbbells per structural slab reaches its maximum of  $1/3$  [5] either globally or locally. This

**Table 2**

Structural parameters of  $\text{YCu}_{6.576}$  (TbCu<sub>7</sub>-type,  $P6/mmm$ ) as obtained by Rietveld synchrotron (S), pair distribution function (model **1:5H**) synchrotron (PDF), neutron (N) and X-ray single crystal (SC) data analyses. Occupancy factors were set as follows:  $1a$ :  $1 - s$ ,  $2c$ :  $1 - 3s$ ,  $3g$ :  $1$ ,  $2e$ :  $s$ ,  $6l$ :  $s$ , where  $s$  corresponds to the concentration of  $\text{Cu}_2$  dumbbells on the Y1a site. Refined values of  $s$  are given in Table 1.

Atom	Data	Site	$x$	$y$	$z$	$B_{\text{iso}}/B_{\text{eq}} [\text{\AA}^2]$
Y1a	S	1a	0	0	0	1.07(2)
	PDF					2.22(1)
	N					1.21(6)
	SC					1.69(6)
Cu2e	S	2e	0	0	0.2870(6)	1.90(6)
	PDF				0.2722(2)	3.7(1)
	N				0.2925(9)	1.0(9)
	SC				0.289(3)	1.2(2)
Cu2c	S	2c	1/3	2/3	0	0.60(3)
	PDF					2.40(1)
	N					0.31(8)
	SC					1.5(1)
Cu6l	S	6l	0.2948(2)	2x	0	1.09(4)
	PDF		0.2810(2)			4.00(2)
	N		0.2940(5)			0.83(8)
	SC		0.298(1)			1.4(1)
Cu3g	S	3g	1/2	0	1/2	1.25(1)
	PDF					2.23(1)
	N					1.08(1)
	SC					1.58(6)

conclusion justifies the choice of the refinement box for the PDF analysis as built from the close packed **2:17** structural slabs (fully or partially ordered) in hexagonal  $ab$  or rhombohedral  $abc$  stacking.

The refined dumbbell concentration  $s$  obtained from the single crystal agrees within the precision limits with the values obtained by Rietveld and PDF analysis of bulk samples (Table 1) and also with the nominal composition. The difference between the lattice parameters obtained from the Rietveld and single crystal data analyses can be understood in terms of systematic errors in the sample-to-detector distance of the single crystal diffractometer.

#### 3.2. Local structure of $\text{YCu}_{6.576}$ from the PDF analysis of total scattering

First we have modeled the structure in the **1:5H** refinement box. The PDF refinement started from the position of all atoms resulting

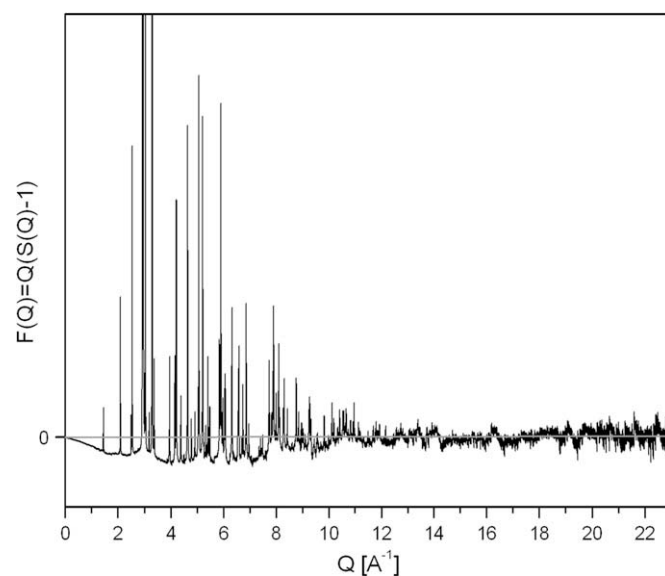


**Fig. 5.** Reduced structure function  $F(Q) = Q[S(Q) - 1]$  as obtained from the SLS synchrotron powder data,  $Q_{\text{max}} = 23 \text{ \AA}^{-1}$ .

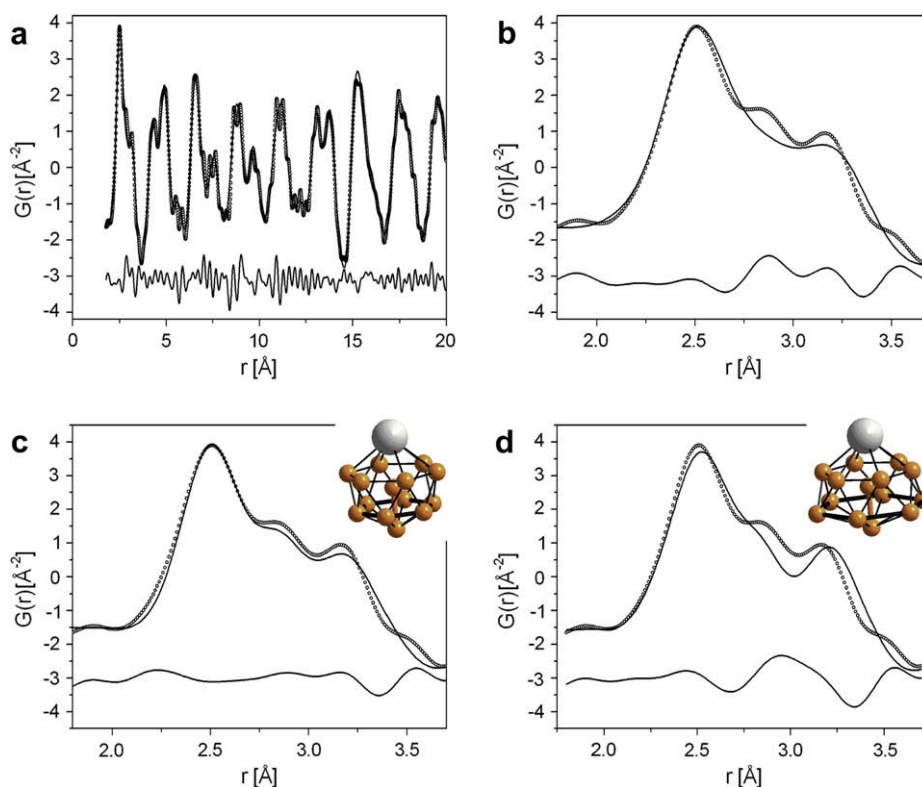


**Fig. 6.** Pair distribution function refinement plot (reduced pair distribution function  $G$  against the distance  $r$ ;  $Q_{\max} = 23 \text{ \AA}^{-1}$ ). Observed as dots, calculated as solid line. The difference curve is shown at the bottom. Upper (a, b): model **1:5H**, bottom (c, d): model **2:17H**; (c) shrinking and (d) expanding the  $\text{Cu}_6$ -hexagon around a  $\text{Cu}_2$  dumbbell (see insets).

from the Rietveld refinement with the exception of the hexagon of Cu atoms around the  $\text{Cu}_2$  dumbbell. These atoms were located at the beginning of the refinement in the average positions corresponding to the  $2c$  site of the **1:5H** structure. The shift of these atoms from the site  $2c$  towards the  $6l$  site (**1:5H**  $P6/mmm$  subcell) was constrained to follow the point symmetry  $-6m2$  of the site  $2c$ , and the occupation of the  $6l$  site was constrained to follow the concentration of dumbbells. The observed PDF was relatively well reproduced by the calculated function (see Fig. 6). The Cu atoms were clearly shifted from  $2c$  to  $6l$  site. The direction of the shifts (towards or from the dumbbell) cannot be, however, elucidated from the refinement in the **1:5H** box, because the refinement box accommodates only one mixed site for Y and  $\text{Cu}_2$  dumbbells. The closer inspection of the PDF refinement plot shows that the observed curve is not well reproduced in the interval  $r = 2.8\text{--}3.2 \text{ \AA}$  (see Fig. 6b) which corresponds to the distances between Cu atoms on the sites  $2e$  and  $6l$ . When shrinkage of hexagon from Cu atoms on  $6l$  position occurs, the distance should be  $\sim 2.8 \text{ \AA}$ , in the case of expansion the distance should be  $\sim 3.2 \text{ \AA}$ .

The next step was therefore the refinement in the **2:17H** box (Fig. 3). The refinement started again from the position of all atoms resulting from the Rietveld refinement with the hexagon of Cu atoms around the  $\text{Cu}_2$  dumbbell located in the average positions corresponding to the  $2c$  site of the **1:5H** ( $P6/mmm$ ) structure (corresponding to sites  $2b$ ,  $2c$  or  $2d$  in the space group  $P6_3/mmc$  of the **2:17H** structure). The shift of these atoms to the position corresponding to the  $12j$  position in the space group  $P6_3/mmc$  was again constrained to follow the point symmetry  $-6m2$ , and the occupation was constrained to follow the concentration of dumbbells. No other constraints were introduced concerning the direction of the shift, towards or from the dumbbell. In all refinement runs the hexagon of Cu atoms converged to the positions corresponding to its shrinkage around the  $\text{Cu}_2$  dumbbell, the observed PDF was well

reproduced including the interval  $r = 2.8\text{--}3.2 \text{ \AA}$  (see Fig. 6c) and the refined dumbbell concentration (Table 1) agrees within the experimental error with the Rietveld analysis. To check the resolution of the observed PDF with respect to the shrinkage or expansion of the  $\text{Cu}_6$  hexagon we have calculated the PDF of the structural model  $\text{Cu}_6$  hexagon expanded by the same amount as the refined shrinking. The clear discrepancy with the observed PDF can be easily seen (compare Fig. 6c to Fig. 6d). These results prove the fact that the direction of the correlated shift of Cu atoms around a  $\text{Cu}_2$  dumbbell in the disordered structure of  $\text{YCu}_{6.576}$  with the **1:5H** structure type is towards the dumbbell as it is the case in the fully ordered **2:17H** structures of similar intermetallic compounds.

Subsequent refinement in the **2:17R** box with the same constrains as in the **2:17H** case resulted in the fit of similar quality as **2:17H** box. Both fits, **2:17H** and **2:17R**, are comparable with the **1:5H** fit for the distances  $r > 3.2 \text{ \AA}$ . It means that we cannot give an answer which type of stacking (*abab* or *abcabc*), if any, is locally realized in the disordered structure of  $\text{YCu}_{6.576}$ . Additional refinement runs in a  $2a$ ,  $2a$ ,  $3c$  supercell of the **1:5H** box on models containing different dumbbell–dumbbell vectors did not reveal any preferred order either. As the results of the PDF refinements we present therefore the **1:5H** refinement for the lattice parameters and atomic parameters (Table 2), and for the interatomic distances within coordination polyhedron of each atom (Table 3) the results of the **2:17H** refinement. These distances are systematically longer than those obtained from the Rietveld analysis of synchrotron and neutron data, which on the other hand agree one with another within the precision limit (when the SCOR correction is applied). The distances obtained from the single crystal analysis are systematically longer. The reason of longer distances as obtained from the PDF analysis and from the single crystal analysis is clearly longer lattice parameters as refined from the PDF and single crystal. The systematic errors in the single crystal results were discussed

**Table 3**

Selected interatomic distances (Å) within the coordination polyhedra for  $\text{YCu}_{6.576}$  as obtained by Rietveld synchrotron (S), pair distribution function (atomic coordinates from **2:17H**, lattice parameters from **1:5H** refinements) synchrotron (PDF), neutron (N) and X-ray single crystal (SC) data analyses. The selection of the distances corresponds to the distances realized locally within the **2:17H** box (Fig. 3).

Y1a	2Cu2e	2.950(2)	S	Y1a'	2Cu2e	2.950(2)	
		3.025(7)	PDF			3.025(7)	
		2.926(6)	N			2.926(6)	
	6Cu6l	2.96(1)	SC		6Cu2c	2.96(1)	
		3.044(1)	S			2.865(1)	
		3.12(1)	PDF			2.869(9)	
		3.047(3)	N			2.864(1)	
		3.034(8)	SC			2.8713(7)	
		3.231(1)	S			3.231(1)	
	12Cu3g	3.239(9)	PDF		12Cu3g	3.239(9)	
		3.230(1)	N			3.230(1)	
		3.2423(6)	SC			3.2423(6)	
Cu2c	3Y	2.865(1)	S	Cu3g	4Y	3.231(1)	
		2.869(9)	PDF			3.239(9)	
		2.864(1)	N			3.230(1)	
		2.8713(7)	SC			3.2423(6)	
	3Cu2c	2.865(1)	S			2Cu2c	2.516(1)
		2.864(1)	N				2.515(1)
		2.869(9)	PDF	2.525(9)			
		2.8713(7)	SC	2.5279(5)			
	6Cu3g	2.516(1)	S	2Cu6l	2.718(1)		
		2.525(9)	PDF		2.81(1)		
		2.515(1)	N		2.722(3)		
		2.5279(5)	SC		2.733(6)		
					4Cu3g	2.482(1)	
						2.485(9)	
				2.481(1)			
				2.4867(6)			
	Cu6l	2Y	3.044(1)	S	Cu2e	Y	2.950(2)
			3.12(1)	PDF			3.025(7)
3.047(3)			N	2.926(6)			
3.034(8)			SC	2.96(1)			
2Cu2e		2.799(1)	S	Cu2e	2.375(4)		
		2.670(5)	PDF		2.263(6)		
		2.801(3)	N		2.41(1)		
		2.84(1)	SC		2.41(2)		
2Cu6l		2.535(1)	S	6Cu6l	2.799(1)		
		2.419(8)	PDF		2.670(5)		
		2.526(3)	N		2.801(3)		
		2.57(1)	SC		2.84(1)		
4Cu3g		2.443(1)	S	6Cu3g	2.633(1)		
		2.436(8)	PDF		2.659(3)		
		2.440(3)	N		2.625(3)		
		2.459(2)	SC		2.637(4)		
2Cu3g		2.718(1)	S				
		2.81(1)	PDF				
		2.722(3)	N				
		2.733(6)	SC				

above. Lattice parameters from PDF analyses are of inferior quality compared to those obtained from Bragg-peak positions due to different treatments of the instrumental resolution function in both analyses; see e.g. [18] or [26].

We can thus conclude about the values of interatomic distances as refined from the Bragg intensities obtained from the synchrotron powder diffraction: The shift of Cu atoms from 2c to 6l site is of 0.33(1) Å. The interatomic distance in the  $\text{Cu}_2$  dumbbell is 2.38 Å, and the other Cu–Cu distances from the first coordination sphere of each Cu atom from the dumbbell are within 2.63–2.80 Å (see Fig. 1f). The shortest interatomic distance in the  $\text{Cu}_6$  hexagon around the dumbbell is within 2.54 Å, and other Cu–Cu distances from the first coordination sphere of each Cu atom from the hexagon are within 2.44–2.80 Å. Compared to the Cu–Cu distance of 2.56 Å in the metallic copper it shows a strong Cu–Cu bonding within the dumbbell and metallic copper like bonding within the  $\text{Cu}_6$  hexagon around the dumbbell.

### 3.3. Dumbbell packing in the structures derived from **1:5H**

The upper limit in the composition of ordered or disordered structures derived from  $\text{CaCu}_5$  type which have only one dumbbell replacing *A* atoms which are not neighbors is  $s = 1/3$  [5]. This in turn corresponds to the composition 2:17. A crystal from the system Yb–Fe–Al [27] with the structure type **1:5H** has the refined composition nearly exactly 2:17, shows no superstructure reflections, no atomic relaxation of *B* atoms towards the 12*p* site and is therefore built up from closely packed slabs with dumbbell concentration of 1/3 and the slabs are randomly stacked. Therefore only the first neighbor condition must be probably fulfilled between the slabs: the stacking *aa* is not allowed: Due to steric effects two  $B_2$  dumbbells cannot follow each other within a chain perpendicular to the slab similarly as in fully ordered **2:17** structures. In the fully disordered structures (**1:5H** type) with the lower concentration of dumbbells than 1/3, like the sample studied here ( $s = 0.19$ ), the structures can be built up either from the slab with the dumbbells concentration of 1/3 and slabs with lower concentration which are randomly stacked or from the slabs with uniform dumbbells concentration lower than 1/3. The PDF modeling points to no *inter-layer* correlation other than the absence of *aa*-type stacking.

In the crystals containing more than 1/3 of  $B_2$  dumbbells on the *A* atom site, locally adjacent dumbbells must exist, and the atomic relaxation of *B* atoms towards the 12*p* site should be observed. No disordered crystals (**1:5H**) with the dumbbell concentration higher than 1/3 were observed in this or other works. On the other hand some crystals with the  $\text{LuFe}_{9.5}$  structure type (**2:17H** cell) having dumbbells concentration higher than 1/3 showed atomic relaxation of *B* atoms towards the edge of the triangle (12*p* site of the **1:5H** subcell) as observed in Refs. [8] and [27].

To complete the discussion, we refer to the series of the structures derived from the  $\text{CaCu}_5$ -type structure by the substitution of the *A* atom by a  $B_2$  dumbbell as it was described in Ref. [28]. The series formula is  $A_{m-n}B_{5m+2n}$ , where *m* denotes the number of  $\text{CaCu}_5$ -type units making up the new structure, and *n* is the total number of *A* atoms being replaced in those *m* units by  $B_2$  dumbbells. Other known ordered structures from this series with the composition different than 1:5 or 2:17 are those of  $\text{ThMn}_{12}$ -type ( $I4/mmm$ ,  $a' = \sqrt{3}a$ ,  $b' = a$  [29]),  $\text{Nd}_3(\text{Fe,Ti})_{29}$ -type [30] and  $\text{Tb}_4(\text{Fe,Si})_{41}$  or  $\text{Tb}_{12}(\text{Fe,Si})_{109}$  compounds [31]. Note that in these structure types with an ordered  $B_2$  dumbbells distribution on the idealized structural slabs (originally basal planes of  $\text{CaCu}_5$  type) the  $B_2$  dumbbells are not hexagonally packed. However, also in this series the *B* atoms of the first coordination sphere around a  $B_2$  dumbbell show the shrinkage towards the dumbbell, as it was now proved experimentally for disordered hyperstoichiometric  $\text{AB}_{5+x}$  for the first time.

## 4. Conclusions

Four independent scattering data analyses, three based on Bragg scattering and one on total scattering, using three different scattering data sets, powder synchrotron, powder neutron and X-ray single crystal, provided consistent structural results on  $\text{YCu}_{6.576}$ . It adopts the  $\text{TbCu}_7$  structure type as a disordered substitution variant of the  $\text{CaCu}_5$  type where  $\text{Cu}_2$ -dumbbells replace *Y* atoms. The local structure around the  $\text{Cu}_2$  dumbbells, as reflected in the diffuse intensity contained in the synchrotron powder data, was correctly modeled using the pair distribution function (PDF) analysis. The resulting model is built as stacking of structural slabs (originally basal planes of  $\text{CaCu}_5$  type) containing hexagonally packed  $\text{Cu}_2$  dumbbells partly substituting *Y* atoms either in the ordered (dumbbells concentration of 1/3) or disordered (dumbbells

concentration lower than 1/3) way. The local stacking of the slabs has to be described in a **2:17** cell, however, both the hexagonal (*ab*) or rhombohedral (*abc*) type are suitable. Therefore a local combination of both stackings that does not possess translational symmetry has been verified by PDF analysis.

Moreover, the PDF analysis confirmed the model of the shrinkage of the Cu<sub>6</sub> atom hexagon in the immediate vicinity of the Cu<sub>2</sub> dumbbell in the **1:5H** structure as it is the case in the ordered superstructures like **2:17H** and **2:17R**.

### Acknowledgements

The assistance of Wouter van Beek (Swiss-Norwegian Beam Lines, ESRF Grenoble) and Fabia Gozzo (Swiss Light Source, PSI Villigen) during synchrotron data collections is highly appreciated. One of us (SB) acknowledges support from the 6th FP European Network of Excellence “Complex Metallic Alloys” as well as the funding of the Deutsche Forschungsgemeinschaft (DFG). The discussion with Simon J.L. Billinge (Columbia University, N.Y.) on the scaling of the observed PDF was indispensable for this work. This work was supported by the Swiss National Science Foundation.

### References

- [1] Haucke W. Kristallstruktur von CaZn<sub>5</sub> and CaCu<sub>5</sub>. *Z Anorg Allg Chem* 1940;244:17–22.
- [2] Guéinée L, Yvon K. Structure stability maps for intermetallic AB<sub>5</sub> compounds. *J Alloys Compd* 2003;356–357:114–9.
- [3] Florio JV, Baenziger NC, Rundle RE. Compounds of thorium with transition metals. II. Systems with iron, cobalt and nickel. *Acta Crystallogr* 1956;9:367–72.
- [4] Makarov ES, Vinogradov SI. Crystal structure of Th<sub>2</sub>Zn<sub>17</sub> and U<sub>2</sub>Zn<sub>17</sub>. *Sov Phys Crystallogr* 1956;1:499–505.
- [5] Filinchuk YE, Birkedal H, Černý R, Hostettler M, Yanson TI, Bodak OI, et al. Chemical heterogeneity of a crystal built of nanoscale coherently twinned Yb<sub>2–x</sub>(Fe, Ga)<sub>17+2x</sub> polytypes. *Chem Eur J* 2004;10:2972–6.
- [6] Buschow KHJ, Van der Goot AS. Intermetallic compounds in the system samarium–cobalt. *J Less-Common Met* 1968;14:323–8.
- [7] Buschow KHJ, Van der Goot AS. Composition and crystal structure of hexagonal Cu-rich rare earth–copper compounds. *Acta Crystallogr* 1971;27B:1085–8.
- [8] Givord D, Lemaire R, Moreau JM, Roudaut E. X-ray and neutron determination of a so-called Th<sub>2</sub>Ni<sub>17</sub>-type structure in the lutetium–iron system. *J Less-Common Met* 1972;29:361–9.
- [9] Ray AE. The crystal structure of CeFe<sub>7</sub>, PrFe<sub>7</sub>, NdFe<sub>7</sub> and SmFe<sub>7</sub>. *Acta Crystallogr* 1966;21:426–30.
- [10] Hornstra J, Buschow KHJ. The crystal structure of YbCu<sub>6.5</sub>. *J Less-Common Met* 1972;27:123–7.
- [11] Ono Y, Shiomi J, Kato H, Iriyama T, Kajitani T. X-ray diffraction study of Sm<sub>2</sub>(Fe<sub>1–x</sub>Al<sub>x</sub>)<sub>17</sub> single crystals with x=0.058, 0.081. *J Magn Magn Mater* 1968;187:113–6.
- [12] Givord D, Laforest J, Schweizer J, Tasset F. Temperature dependence of the samarium magnetic form factor in SmCo<sub>5</sub>. *J Appl Phys* 1979;50(3):2008–10.
- [13] Joubert JM, Černý R, Latroche M, Leroy E, Guéinée L, Percheron-Guégan A, et al. A structural study of the homogeneity domain of LaNi<sub>5</sub>. *J Solid State Chem* 2002;166:1–6.
- [14] Gulay LD. Investigation of phase diagram of the Y–Cu–Pb system at 870 K. *J Alloys Compd* 2000;313:144–7.
- [15] Egami T, Billinge SJL. *Underneath the Bragg-peaks: structural analysis of complex materials*. Oxford: Pergamon Press; 2003.
- [16] Brühne S, Sterzel R, Uhrig E, Gross C, Assmus W. Medium range real atomic structure of face-centred icosahedral Ho<sub>9</sub>Mg<sub>26</sub>Zn<sub>65</sub>. *Z Kristallogr* 2004;219:245–58.
- [17] Brühne S, Uhrig E, Gross C, Assmus W, Masadeh AS, Billinge SJL. The local atomic quasicrystal structure of the icosahedral Mg<sub>25</sub>Y<sub>11</sub>Zn<sub>64</sub> alloy. *J Phys Condens Matter* 2005;17:1561–72.
- [18] Feuerbacher M, Makongo JPA, Hoffmann S, Cardoso R, Grin Yu, Kreiner G, et al. The samson phase, β-Mg<sub>2</sub>Al<sub>3</sub>, revisited. *Z Kristallogr* 2007;222:259–88 [chapter 6.1].
- [19] Schmitt B, Brönnimann Ch, Eikenberry EF, Gozzo F, Hörmann C, Horisberger R, et al. Mythen detector system. *Nucl Instrum Met Phys Res A* 2003;501:267–72.
- [20] Rodríguez-Carvajal J. Recent developments of the program FULLPROF. *IUCr CPD Newsletter* 2001;26:12–9.
- [21] Sheldrick G. SHELXL97: program for crystal structure refinement. Germany: University of Göttingen; 1997.
- [22] Qiu X, Thompson JW, Billinge SJL. PDFgetX2: a GUI-driven program to obtain the pair distribution function from X-ray powder diffraction data. *J Appl Crystallogr* 2004;37:678.
- [23] Farrow CL, Juhas P, Liu JW, Bryndin D, Božin ES, Bloch J, et al. PDFfit2 and PDFgui: computer programs for studying nanostructure in crystals. *J Phys Condens Matter* 2007;19:335219.
- [24] Bérar JF, Lelann P. E.s.d.'s and estimated probable error obtained in Rietveld refinements with local correlations. *J Appl Crystallogr* 1991;24:1–5.
- [25] Pawley GS. EDINP, the Edinburgh powder profile refinement program. *J Appl Crystallogr* 1980;13:630–3.
- [26] Qiu X, Božin ES, Juhas P, Proffen T, Billinge SJL. Reciprocal-space instrumental effects on the real-space neutron atomic pair distribution function. *J Appl Crystallogr* 2004;37:110–6.
- [27] Černý R, Pacheco V, Yanson TI, Manyako M, Bodak OI. Structure of iron-rich compounds in the Yb–Fe–Al system. *Z Kristallogr* 2003;218:802–10.
- [28] Stadelmaier HH. Structure classification of transition metal–rare earth compounds between T and RT<sub>5</sub>. *Z Metallkd* 1984;75:227.
- [29] Florio JV, Rundle RE, Snow AI. Compounds of thorium with transition metals. I. The thorium–manganese system. *Acta Crystallogr* 1952;5:449–57.
- [30] Psycharis V, Kalogirou O, Niarchos D, Gjoka M. Ab initio crystal structure solution of the novel intermetallic compound Nd<sub>3</sub>(Fe, Ti)<sub>29</sub>. *J Alloys Compd* 1996;234:62–6.
- [31] Ivanova GV, Makarova GM, Shcherbakova YeV, Belozherov YeV. New phases in Tb–Fe–Si system. *J Alloys Compd* 2000;309:141–6.
- [32] Petkov V, Billinge SJL, Heising J, Kanatzidis MG. Application of atomic pair distribution function analysis to materials with intrinsic disorder. three-dimensional structure of exfoliated-restacked WS<sub>2</sub>: not just a random turbostratic assembly of layers. *J Am Chem Soc* 2000;122:11571–6.